applied sciences

MDPI

Article

Fiber-Optic System for Monitoring Pit Collapse Prevention

Yelena Neshina [1], Ali Mekhtiyev [2,*], Valeriy Kalytka [1], Nurbol Kaliaskarov [1], Olga Galtseva [3,*] and Ilyas Kazambayev [2]

[1] Faculty of Energy, Automation and Telecommunications, Abylkas Saginov Karaganda Technical University, Karaganda 100012, Kazakhstan; 1_neg@mail.ru (Y.N.); manuscript.kz@bk.ru (V.K.); 90nurbol@mail.ru (N.K.)
[2] Operating Electra Equipment Department, Saken Seifullin Kazakh Agro Technical Research University, Astana 010011, Kazakhstan; ilyaskazambayev@gmail.com
[3] School of Non-Destructive Testing, National Research Tomsk Polytechnic University, Tomsk 634050, Russia
* Correspondence: barton.kz@mail.ru (A.M.); piano@tpu.ru (O.G.); Tel.: +7-913-800-15-50 (O.G.)

Abstract: Currently, there are many enterprises involved in extracting and processing of primary raw materials. The danger of working in this industry consists in the formation of cracks in rocks of the pit side slopes, which can lead to destruction. This article discusses the existing systems for monitoring the pit collapse prevention. The most promising is the use of systems with fiber-optic sensors. However, use of these systems is associated with some difficulties due to high costs, low noise immunity, and in some cases, the requirement for additional equipment to improve the reliability of measurements. A completely new method of processing the data from a fiber-optic sensor that simplifies the design and reduces the cost of the device is proposed considering the experience of previous developments. The system uses artificial intelligence, which improves the data processing. The theoretical part is dedicated to the development of foundations, and the analysis of the nonlinear properties of the physical and mathematical model of optical processes associated with the propagation of an electromagnetic wave in a fiber-optic material was developed. The results of experimental and theoretical applied research, which are important for the development of fiber-optic systems for monitoring the pit collapse prevention, are presented. The dependences of optical losses and the number of pixels on the dis-placement were obtained. The accuracy of the method corresponds to the accuracy of the device by which it is calibrated and is 0.001 mm. The developed hardware-software complex is able to track the rate of changing the derivative of the light wave intensity in time, as well as changing the shape of the spot and transition of pixels from white to black.

Keywords: fiber-optic sensor; optical fiber; pit structural monitoring; optical losses; light spot; pixel amounts

Citation: Neshina, Y.; Mekhtiyev, A.; Kalytka, V.; Kaliaskarov, N.; Galtseva, O.; Kazambayev, I. Fiber-Optic System for Monitoring Pit Collapse Prevention. *Appl. Sci.* **2024**, *14*, x. https://doi.org/10.3390/xxxxx

Academic Editor: Detlef Kip

Received: 3 April 2024
Revised: 23 May 2024
Accepted: 24 May 2024
Published: date

1. Introduction

In the last 10–15 years, control and measuring instruments, devices (sensors, hardware and software components for computers, sensors, etc.) and process monitoring systems have used automated high-speed functional elements and circuits based on fiber-optic materials (FOM). They have caused significant applied scientific and technical interest for a number of branches of modern industry: laser technology, microelectronics and radio electronics, mining technologies and metallurgy, non-destructive testing technologies and resistance of materials, mechanical engineering, aircraft building and rocket science, etc., first of all, because of organizing high-quality electronic measurements with a high degree of accuracy of results (often in real time and with remote access) when monitoring the technical conditions (deformation and mechanical stress parameters) of extended large-scale objects (dams, bridges, embankments, mining pits, etc.) [1]. A possible solution is to build systems using fiber-optic sensors. Moreover, the advantages of fiber-optic control and measuring systems have been known for a long time. For example, they

are not affected by electromagnetic interference (noise); they have high electric physical (nonlinear relaxation polarization and conductivity), optical (nonlinear electric optical phenomena) and metrological characteristics; they have distributed and quasi-distributed sensitivity; they are able to work in an explosive environment. At the same time, the measuring channels have a significant length, and the cost of fiber-optic conductors is lower than that of copper ones; every year, the cost of optical fiber (OF) is reduced, and its properties are improved. Another feature of using fiber-optic sensors (FOS) is their low power consumption and the ability to work at a considerable distance from the data processing unit, since the light signal is weakly attenuated, unlike the electric one. In addition, OFs do not oxidate [2]. OFs can be used to build distributed and quasi-distributed measuring systems for monitoring geotechnical parameters and the safety of mining operations in pits and coal mines [3], as well as the other extended objects. Security systems for perimeters and borders of various types and purposes have been developed based on the FOS [4]. FOS are actively used in the aerospace and oil and gas industries [5], since they have significant advantages over electrical sensors based on the clarity of the physical principle of operation and their positive properties, which ensure their large-scale implementation. Sufficiently serious scientific work has been carried out in the field of improving the safety of open-cast marble extraction [6].

There are image surveillance systems, Global Positioning System (GPS) technologies, ultrasonic measurements, specialized sensors and IoT-applications [7], according to the analyzed literature, that are used in order to monitor the technical condition of concrete, metal structures. Moreover, FOS are widely used [8]. The reasons for the development were the decrease of the materials cost and improvements in measurement tools [9]. The main methods of measuring external impacts include Tunable Wavelength Coherent Optical Time Domain Reflectometry (TW-COTDR), Phase Shift Pulse Brillouin Optical Time Domain Reflectometry (PSP-BOTDR), Pulse-Prepump Brillouin Optical Time Domain Analysis (PPP-BOTDA), Brillouin Optical Time Domain Analysis (BOTDA), Brillouin Optical Time Domain Reflectometry (BOTDR), Optical Frequency Domain Reflectometry (OFDR) or methods based on measuring losses in an OF caused by Brillouin scattering [10]. Moreover, the most widely used among FOS sensors are those built on Bragg gratings, with the measurement of losses by scattering of Brillouin, Raman, Rayleigh [11]. It should be noted that the main advantage of OF is the ability to measure not only one parameter but also two interrelated parameters [12,13], for example, displacement and mechanical stress or two parameters with a low correlation, such as temperature and mechanical stress [14,15], and in some cases, three parameters [16]. However, this application requires large computing power or more complex designs. In the case of point-by-point measurement application, the presence of corrosion on steel reinforcement can also be monitored [17]. On the other hand, it is possible to measure the force exerted by rock displacement using a point-by-point fiber-optic sensor [18]. The advantages of this solution are high measurement accuracy, as well as compensation for signal interference caused by temperature changes. Despite this, the quality of the welding of the sensing element can greatly affect the measurement, while the welding itself complicates the mounting and dismantling processes. Another possible solution to this problem in measuring stress can be a device made in the form of a metal ring, on which Bragg gratings, a polling device and a controller based on a Field-Programmable Gate Array (FPGA) are mounted [19]. The special design of the device provides high accuracy and linear dependence of measurements; the controller provides temperature compensation. However, the above options have a high cost and a complex design.

Another case of using FOS is to determine the increase of the displacements of rocks, stone slabs, for example, [12]. This solution is made in the form of a special design mounted in a metal box. The principle of operation is to measure the angle of inclination along the wavelength. The advantages are the accuracy of crack measurement, detuning from the temperature changes. The disadvantages are the design complexity and high

cost. On the other hand, a temperature-compensated sensor can be considered, which consists of a cable made using a multi-mode fiber, an input and output single-mode fiber and is made in the form of a spiral [20]. The advantages of the device are an increased measurement accuracy and temperature compensation. The disadvantages are the absence of the consideration of the vibrations effect on readings, as well as high requirements for equipment to correct the error caused by temperature changes.

It should be noted that the use of FOS makes it possible to monitor the integrity of mines. For example, there is information about developing a system for monitoring rock displacement and preventing the collapse of mine workings in coal mines in China [21]. Fiber-optic vertical and horizontal seismic receivers based on a Mach–Zehnder interferometer have been considered. Authors have proposed an original design of a sensitive element that provides a high-threshold sensitivity of the measuring device to seismic accelerations. Stability of the Mach–Zehnder interferometer operation is ensured using an active stabilization system for the operating point [22]. Developing their area, the authors proposed their own construction that has certain common features with those considered earlier in [23,24].

On the other hand, increasing the sensitivity of fiber-optic interferometric sensors is achieved using a multi-turn sensitive functional element (acting element), in which the FOS is based on a two-arm Mach–Zehnder interferometer [25]. The theoretical basis for the development of long-baseline strainmeters was work [26] that presented the results of studying long-baseline strainmeters designed to monitor the mechanical states of large-scale objects. In this work, there was partially solved the important problem of reducing the fading of the strainmeter output signal with change of the external temperature. Although the use of a multi-turn sensing element in the design of FOS can significantly improve the performance of FOS in strain measurements, it was not possible to completely eliminate the temperature negative effect (the effects of thermal elasticity) on the measurement process. The decrease in the drift of the operating point of the interferometer due to the spatial localization of the interferometer while maintaining the length of the measuring base was observed. In addition, there is no information about testing a prototype in the field, so it cannot be argued that the proposed FOS is able to reduce the deviation of the output signal over time compared with the traditional electromechanical sensor from 12% to 2%. Only a functional diagram of a long-based strainmeter was presented, and the absence of photographs of a prototype can demonstrate the incompleteness of the studies and the absence of empirical data obtained as a result of studying full-scale FOS samples. Since there are no results of testing the FOS under conditions of changing the external temperature, it is impossible to unequivocally assert its effectiveness and complete solution of such an important problem for this device.

It is known that the drift of the operating point can begin when the temperature changes within 1 °C [27], so there is a change in the intensity of the incident light wave on the surface of the photodetector. First of all, the phase of propagation of the light wave changes. The authors also did not indicate which fiber they used, since there are significant differences between the application of the multi- and single-mode OF [28]. The relative sensitivity of a strainmeter with a multi-turn sensitive element depends on the coefficient of elasticity k. The use in the FOS of a Mach–Zehnder interferometer is accompanied by the risk of the strainmeter output signal fade and the appearance of false signals about the displacement of rocks [26–30]. The rejection of a rather complex design that requires fine-tuning will significantly increase the FOS reliability.

It should be noted that the high sensitivity of Distributed Fiber-Optic Sensors (DFOS) is an advantage of such devices and a cause of measurement interference. In order to achieve high accuracy, such devices are used with machine learning systems [31]. Signal processing is most often carried out by constructing two-dimensional graphs; however, there are methods of identifying damage using a three-dimensional transformation [32]. In another case, for example, for signal processing with the use of PPP-BOTDA, artificial intelligence based on the Random Sample Consensus (RANSAC) method [33] is used.

Moreover, the use of neural networks, for example, convolutional neural networks (CNN), makes it possible to process the optical signal with high accuracy [34]. Such systems make it possible to increase the accuracy of measuring three-dimensional mechanical stresses, but at the same time, the disadvantages are the large size and cost of the equipment, as well as the complexity of information processing.

Therefore, reducing the cost to develop a fiber-optic system will make it possible to use it in more facilities. This article presents a solution using a camera to track changes in a spot of light. In previous works on the development of a mine support pressure monitoring system [35,36], it was found that not only the optical signal should be processed but also the electrical signal that supplies power to the optical radiation generator. At the same time, in attempts to develop a hardware-software complex, the elements of machine learning were used, which made it possible to distinguish noise in a signal when external impacts were exerted by such factors as the movement of a person or a machine [37]. These sources contain a detailed description of the main technical solution and all the advantages of the proposed system. Thus, this work proposes tracking crack displacements by such a parameter as the number of pixels of optical signal loss using a photomatrix, which is a fundamental difference from existing data processing methods using hardware-software complex algorithms to reduce external interference.

2. Materials and Methods

Let us assume that the geometric model of the main working element of an optical fiber (OF) is in the form of a cylindrical sample with a base radius r_0 and length l. The refractive index of material of the fiber-optic element is accepted in the general case $n = \frac{k}{k_0} = \frac{c}{\vartheta} = \frac{\lambda_0}{\lambda}$, where $k_0 = \frac{\omega}{c} = \frac{2\pi}{\lambda_0}$; $k = \frac{\omega}{\upsilon} = \frac{2\pi}{\lambda}$ k $= \frac{\omega}{\vartheta} = \frac{2\pi}{\lambda}$ are the wave vectors of the falling and refracted waves, respectively.

The physical model of the wave processes studied in the fiber-optic element will be constructed using the methods of classical electrodynamics and wave optics. The parameter of the d'Alembert wave equation for a input wave (falling from air at an angle θ onto the cross-sectional surface of a fiber-optic element) is $\overline{\nabla^2}\,\vec{u} - \frac{1}{c^2}\frac{\partial^2\vec{u}}{\partial t^2} = 0$, and wave, refracted at an angle γ in the fiber-optic element, is $\overline{\nabla^2}\,\vec{u} - \frac{1}{\upsilon^2}\frac{\partial^2\vec{u}}{\partial t^2} = 0$. Its general solution is taken in the form

$$\frac{1}{c} = \sqrt{\varepsilon_0\mu_0}\ \ ,\vec{u} = \overrightarrow{u_0}\ \ \cdot \exp\left(i\omega t\text{-}\left(\overrightarrow{k_0\vec{r}}\right)\right)\ \ \frac{1}{c} = \sqrt{\varepsilon_0\mu_0}\,;\ \ \overrightarrow{u_0} = \vec{u}_0 \cdot \exp\left(i\omega t - \left(\overrightarrow{k_0\vec{r}}\right)\right).$$

$$\frac{1}{\upsilon} = \frac{k}{k_0 c} \cdot \sqrt{\varepsilon_0\mu_0\varepsilon\mu};\ \ \vec{u} = \vec{u}_0 \cdot \exp\left(i\omega t - \left(\vec{k}\vec{r}\right)\right).$$

Vector classical wave function $\vec{u}(\overrightarrow{r;t})$ is characterized by the amplitude $\overrightarrow{u_0}$ and the spatial phase $\phi = \left(\vec{k}\vec{r}\right) = \frac{\omega}{\vartheta^2}\left(\vec{\vartheta}\vec{r}\right)$.

The vector $\vec{u}(\overrightarrow{r;t})$ acts as both the electric field strength vector $\vec{E}(\overrightarrow{r;t})$ and the wave's magnetic field strength vector $\vec{H}(\overrightarrow{r;t})$. The spatial phase of the falling wave is taken as equal to $\phi_0 = \left(\overrightarrow{k_0\vec{r}}\right) = \frac{\omega}{c^2}(\vec{c}\vec{r})$. The spatial phase of the refracted wave is taken as equal to $\phi_0 = \left(\vec{k}\vec{r}\right) = \frac{\omega}{\upsilon^2}(\vec{\upsilon}\vec{r})$.

The selection of the directions of single vectors $\overrightarrow{\tau_0}$, $\vec{\tau}$ is based on the directions of the rate vectors $\vec{c}$, $\vec{\upsilon}$ and the wave vectors $\vec{k}_0 = \frac{\omega}{c}\overrightarrow{\tau_0}, \vec{k} = \frac{\omega}{\upsilon}\vec{\tau}$. The direction of the $\vec{c}$ vector is based on the radius-vector of the point on the surface of $\vec{r}$ light-sensitive element, accepting $(\overrightarrow{\tau_0}\vec{r}) = r \cdot cos\alpha_1$, $(\vec{\tau}\vec{r}) = r \cdot cos\alpha_2$, $\psi = \theta - \gamma$, $\psi = \alpha_2 - \alpha_1$, the Equation $cos\,\psi = \frac{cos\,\theta(\sqrt{n^2 - sin^2\theta} + sin^2\theta)}{n}$ is obtained.

Then, the spatial difference of these waves phases is $\varphi - \varphi_0 = \frac{\omega}{c^2}(ncos\psi - 1)(\vec{c}\vec{r})$, where $n = \frac{sin\,\theta}{sin\,\gamma}$, r is the distance from the point of intersection of the light beam (a wave

incident on the surface of the cross-section of the optical fiber) with the surface of a given section, placed in this model at the origin of coordinates to a fixed point in space.

Accordingly,

$$\varphi_2\text{-}\varphi_1 = \frac{\omega}{\mathrm{c}}\cos\theta\,(\sqrt{\mathrm{n}^2\text{-}\sin^2\theta}\text{-}\cos\theta)(\overrightarrow{\tau_0}\overrightarrow{\mathrm{r}})\varphi - \varphi_0 = \frac{\omega}{c}cos\,\theta\sqrt{n^2 - sin^2\,\theta} - cos\,\theta)(\overrightarrow{\tau_0}\overrightarrow{r}). \quad (1)$$

Next, based on the developed geometric model, the beam falls from the air at an angle θ onto the cross-sectional surface of the central cable (core) of the fiber-optic element, continuing the beam until it intersects with the side boundary of the element. Let us denote the continuation of the beam in the form of a segment OM_1 and the refracted wave in the form of a segment OM_2. The lengths of the segments are r_1 and r_2; the angle between them is equal to $\psi = \theta - \gamma$.

According to the geometric model, we have $r_2 - r_1 = OM_1(\frac{OM_2}{OM_1} - cos\,\psi)$, where $\frac{OM_2}{OM_1} = \frac{sin\,\theta}{sin\,\gamma}$, $OM_1 = \frac{d}{2sin\,\theta}$, and $r_2 - r_1 = \frac{d}{2sin\,\theta}(n - cos\psi)$. $\mathrm{r_2\text{-}r_1} = \frac{\mathrm{d}}{2\sin\theta}(\mathrm{n}\text{-}\cos\psi)$. Then, $r_2 - r_1 = \frac{d}{2sin\,\theta} \times \frac{n^2 - (cos\,\theta\sqrt{n^2 - sin^2\,\theta} + sin^2\,\theta)}{n}$.

Taking the spatial difference of the phases of the incident and refracted waves in the direction of the $\vec{\tau}$ vector, approximately assuming $\varphi_2 - \varphi_1 = kr_2 - kr_1 \approx \frac{\omega}{c}(r_2 - r_1)\varphi_2\text{-}\varphi_1 = \mathrm{kr_2\text{-}k_0r_1} \approx \frac{\omega}{\mathrm{c}}(\mathrm{r_2\text{-}r_1})$, according to $r_1 = \frac{d}{2sin\,\theta}$, we obtain

$$\varphi_2 - \varphi_1 = \frac{\omega}{c} \times \frac{d}{2nsin\,\theta} \times (n^2 - (cos\,\theta\sqrt{n^2 - sin^2\,\theta} + sin^2\,\theta)). \quad (2)$$

From (1) $cos\,\theta\sqrt{n^2 - sin^2\,\theta} + sin^2\,\theta - 1 = \frac{1}{n} \times (n^2 - (cos\,\theta\sqrt{n^2 - sin^2\,\theta} + sin^2\,\theta))$ or

$$cos\,\theta\sqrt{n^2 - sin^2\,\theta} + sin^2\,\theta = n. \quad (3)$$

Its decision $n = cos\,\theta\sqrt{(1+\sqrt{2})^2 + cos^2\,\theta + sin^2\,\theta} = cos\,\theta\sqrt{(1+\sqrt{2})^2 + tg^2\,\theta}$, formally satisfying this equation from a physical point of view, does not pretend to be strictly scientifically correct and requires a more detailed study primarily in terms of compatibility with the generalized kinetic equation, which describes, at the molecular level, the processes of interaction of an optical signal with a fiber-optic element in a wide range of substance parameters, including the electromagnetic field and temperature.

The theoretical part, presented in this paper, is an exposition of the conceptual theoretical foundations of a physical and mathematical model of electron-optical processes (generally nonlinear) associated with the interaction of a monochromatic electromagnetic wave with the substance of a fiber-optic element under the external conditions established in the model. Obviously, a strict physical model of such processes should be based on solving a kinetic equation that allows calculating the concentrations of optically active centers (atoms, molecules, atomic groups, etc.) that are the centers of scattering of an external optical signal (optical relaxers), as well as excessive (above equilibrium) concentrations of electrically charged particles (electrophysical relaxers) moving under the action of the electric and magnetic fields of the wave in the potential field of the crystal lattice of the model sample, which determines such nonequilibrium processes as relaxation polarization in the visible wavelength range. The solution of the kinetic equation should be constructed in conjunction with Maxwell's equations for the electromagnetic field of the wave in the substance of the fiber-optic material. In general, a comprehensive solution to this problem will require, in the future, the development of quite theoretically complex schemes and methods related, firstly, to the choice of the correct physical methodology for constructing the kinetic equation of electron-optical processes in optical fiber(s), including kinetic coefficients the processes of interaction of an external electromagnetic field (optical signal) with optical centers and electrophysical relaxers describing at the microscopic level. Secondly, it will be necessary to choose a convenient methodology, from the

point of view of comparing the results of theory and experiment, for experimental estimates of the studied microscopic processes (light scattering, electric polarization; light refraction), which will require determining both the list of experimentally determined electrical and optical parameters and the schemes of precision measurements of these parameters. The tasks outlined above are not being set at this stage of research, including in this paper. There is only limit by the description of the conceptual foundations and schemes for the implementation of the nonlinear kinetic theory of electron-optical effects in optical fiber planned in the future.

The main task of the theoretical section is to develop conceptual (corresponding to the schemes and experimental conditions) fundamentals of a physical and mathematical model of optical-electrical processes occurring in a fiber-optic element during its interaction with a monochromatic electromagnetic wave (an optical signal coming from a coherent radiation source) in a wide range of electromagnetic wave parameters and temperature. At the same time, the final analytical relations between the calculated macroscopic parameters of the system will be established by generalized phenomenological methods (without detailing the structure and properties of the kinetic equation and its boundary and initial conditions), and in the meantime, approximate methods (from the point of view of the physical specificity of the dependencies observed in the experiment). The main task in this section is to formulate a final mathematical expression that establishes a connection between the optical characteristics of the process (intensity of the luminous flux, refractive index of the substance) and the experimentally measured electro-optical characteristic of the system under study. It is possible that in the process of clarifying the structure and general appearance of the optical-electric kinetic equation and, when solving it jointly with Maxwell's equations, both intermediate and final equations of the model will appear, which will significantly affect the final calculation formulas. Methodologies and schemes for measuring the electro-optical characteristics of the system will not be developed in this work. The solution of all these issues will be the subject of research in subsequent works based on this preliminary theoretical study.

The comparison of the results of numerical calculations performed according to theoretical formulas and measured in an experiment will not be carried out in this article. The theoretical section is given after the experimental one, since it is of an auxiliary nature and, so far, is not directly compared with the experiment.

The mathematical model of the processes of interaction of an optical signal with the substance of an OF will be built using the expression for the bias current density $\vec{j}(t) = \frac{\partial \vec{D}}{\partial t} = i\omega\varepsilon_0\varepsilon_\infty\vec{E}(t) + \frac{\partial \overrightarrow{P_{rp}}(t)}{\partial t}$ [30], where ε_∞ is an inductive (high-frequency) component of the complex permittivity (CDP), neglecting the relaxation (low-frequency) polarization of the sample $\frac{\partial \overrightarrow{P_{rp}}(t)}{\partial t} \to 0$ [30,31], and calculating the volumetric density of the electromagnetic wave in the optic fiber in the form [32]:

$$P_{Vt} = 2 < Re(\vec{E}(t)) \times Im(\vec{j}(t)) > \approx \omega\varepsilon_0\varepsilon_\infty\vec{E}_0^2. \quad (4)$$

The equation $\mu_0\overrightarrow{H_0^2} = \varepsilon_0\varepsilon_\infty\overrightarrow{E_0^2}$ is used for the electromagnetic wave on the condition $\mu_\infty = 1$ (for non-magnetic material).

The value of the refractive index of a light wave in this model (in the optical and wavelength range) is determined by the high-frequency component of the complex dielectric constant $n_\infty = \sqrt{\varepsilon_\infty}$. The refractive index of OF, in general, can be represented as a multidimensional functional $n_\infty(\varsigma_0; \omega; E_0; T; d; l; \theta; \alpha_0)$, defined on a set of variables representing a set of physical parameters of various types reflecting the properties of the structure and geometry of the experimental sample (fiber-optic element).

First of all, these parameters include:

(1) Microscopic characteristics of the structure or molecular characteristics presented in the form of a set of variables of the model under study $\varsigma_0 = n_\infty(U_0; \nu_0; \delta_0; n_0; a)$ [1],

where U_0 is the activation energy of relaxators (centers of interaction of an electromagnetic wave (optical signal) with matter); ν_0 is the natural oscillation frequency of the relaxator (molecule, ion, cluster) relative to the equilibrium position; δ_0 is the width of the potential barrier overcome by the relaxer due to thermal activation (in this case, as a result of thermal fluctuations that significantly affect optical processes in the fiber in the field of thermoelastic deformations); n_0 is the equilibrium concentration of relaxers (in the absence of external disturbances (electromagnetic fields) in OF); a is the lattice constant (in the case of a crystal structure) [10]. For the first time, the application of the method of minimizing the comparison function in relation to theoretical studies of the kinetics of electro-optical and electrophysical processes in materials of various crystal structure complexity (in particular, in fiber-optic samples) was proposed in [10–14].

(2) Field characteristics: amplitude E_0 and frequency ω of the electromagnetic wave (optical signal) $\vec{E} = \overrightarrow{E_0} \cdot \exp\left(i\omega t - \left(\vec{k}\vec{r}\right)\right)$. In this model, the electric field strength vector of a wave propagating in space with a circular frequency $\omega = \frac{2\pi\upsilon}{\lambda}$ $\omega = \frac{2\pi\nu}{\lambda}$and a wave vector $k = \frac{2\pi}{\lambda}$ is recorded at an arbitrary point in space $\vec{r}$ at time t, according to a generalized solution of the classical Dalembert wave equation $\overline{\nabla^2}\,\vec{E} - \frac{1}{v^2}\frac{\partial^2 E}{\partial t^2} = 0$ for a free electromagnetic field (away from the source).

(3) The third parameter is temperature, the effect of which on almost all kinetic drying is obvious and depends, firstly, on the features of the crystal structure; secondly, on the physical nature of the process; and, thirdly, on the ratios of the energy of the relaxator in the external field and the energy of the thermal motion of the relaxers. The weak influence of temperature changes on electro-optical phenomena is considered in this approximation [30].

(4) Geometric parameters: d is the diameter of the working part (core) of the fiber-optic sample; l is its length.

(5) Optical and geometric characteristics: θ is the angle of incidence of light on the surface of the cross-section of the fiber-optic element; α_0 is the angle between the direction of the light beam coming out of the cross section of the fiber-optic element and the normal vector to the surface of the photosensitive element (plate). The infinity sign in the designation of a multiparametric physical quantity n_∞ means that relaxation electro-optical processes in a fiber-optic element are considered in the optical frequency range.

The calculation of the electromagnetic wave intensity, averaged over the oscillation period of the wave $I = < Re\left[\left|\vec{E}(t)\right|\right) \times Im[|(\vec{H}(t)|] > \approx \frac{1}{2}|\overrightarrow{E_0}||\overrightarrow{H_0}|$ in the approximation $I = \frac{1}{2}\sqrt{\frac{\varepsilon_0\varepsilon_\infty}{\mu_0}}\,\overrightarrow{E_0^2}$, gives the distribution of the volumetric power density of the electromagnetic field of the wave over the angles (between the direction of the wave vector and the normal to the surface of the sensitive light-perceiving plate):

$$P_{Vt} = 2\omega\sqrt{\varepsilon_0\mu_0\varepsilon_\infty}I \approx 2\omega\frac{n_\infty\left(\varsigma_0;\omega;E_0;T;d;l;\theta;\alpha_0\right)}{c}I(\alpha_0). \quad (5)$$

The calculated value $n_\infty(\varsigma_0;\omega;E_0;T;d;l;\theta;\alpha_0)$ is determined from Equation (3).

Rigorous calculation of the optical signal intensity in the OF $I(\varsigma_0;\omega;E_0;T;d;l;\theta;\alpha_0)$ as well as for $n_\infty(\varsigma_0;\omega;E_0;T;d;l;\theta;\alpha_0)$ should be performed by the methods of the nonlinear kinetic theory in combination with the methods of regression analysis, by minimizing the differences between the results of theory and experiment [37]. Solving this issue is a separate complex task beyond the scope of this work and will be carried out in the future.

In general, the value measured in the experiment is function $I(\varsigma_0;\omega;E_0;T;d;l;\theta;\alpha_0)$, averaged by angles α_0. Then

$$< P_{Vt}(\varsigma_0; \omega; E_0; T; d; l; \theta) >= \frac{\omega}{c\pi} \times \int_0^{2\pi} I(\alpha_0)\, n_\infty(\varsigma_0; \omega; E_0; T; d; l; \theta; \alpha_0) d\alpha_0. \quad (6)$$

The numerical processing of expression (6) will be carried out by means of high-speed software and hardware, by direct comparison, in real time, with the experimental picture of the intensity distribution of the output optical signal over the surface of the photodetector plate in the recording device.

The effect of deformations of fiber-optic samples will be taken into account by the methods of perturbation theory [30] by expanding the calculated value measured in the experiment $< P_{Vt}(\varsigma_0; \omega; E_0; T; d; l; \theta) >$ into infinite power series in powers of the dimensionless small strain parameter $\frac{\delta d}{d}$. Zero approximation of perturbation theory with respect to a small parameter $\frac{\delta d}{d}$ in approximation $\frac{\delta(\vec{\tau_0}\vec{r})}{(\vec{\tau_0}\vec{r})_0} \approx \frac{(\delta\alpha)^2}{c2}$ gives the calculated (theoretical) value of the volumetric power density of the electromagnetic field of the wave detected by a sensitive membrane (photographic plate) after refraction of the outgoing (primary optical signal) in an undeformed fiber-optic sample.

2.1. Experimental Installation

The hypothesis assumes the application of a G.652 type single-mode OF as a sensor and data transmission system. Taking into account the length of mine workings, it is necessary to ensure the installation of a FOS at a considerable distance from the data processing unit. The only option to build a distributed monitoring system with low power consumption and signal attenuation is possible only on the basis of OF. To test the theory, a laboratory bench was developed (Figures 1 and 2). The displacement measurements were made by two methods to ensure reliability of the results. Figure 1 shows the first method of controlling the change in the pixels of a light spot that is formed at the exit from the OF and falls on the surface of the television matrix. The second method shown in Figure 2 is based on controlling the additional losses of light waves that appear in the OF during the occurrence of the mechanical impact or the bending.

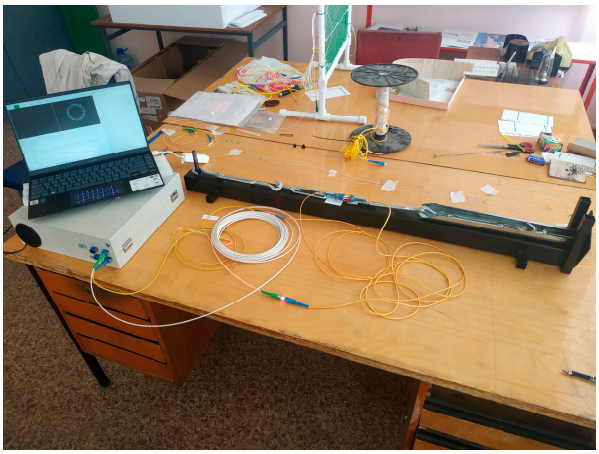

Figure 1. Laboratory bench with the use of the developed HSC.

Figure 2. Laboratory bench with the use of a reflectometer.

In the first case, a solid-state laser from a visual fault locator in an OF was used as a radiation source. An important point was selecting this light source according to the parameters of radiation coherence and its stability, because even radiation frequency deviations of more than 5% lead to a failure in the monitoring system. On the other hand, the sensor was connected to a light source at one end and to a television matrix at the other. Data processing as carried out using a hardware-software complex; the visualization of measurements as represented by graphs on a computer screen.

A VIAVI Smart Pocket OLP-38 optical power meter (JDSU) (Viavi Solutions, San-Jose, CA, USA) was used to determine optical power and loss values. It operates in the dynamic range from −50 to +26 dBm with a wavelength range of 780÷1650 nm and has the ability to automatically estimate the level of optical power without switching the measurement range, as well as to measure the insertion losses formed in the optical conductor when a light wave passes through its core. In addition, a Smart Pocket OLS-34 cogeneration radiation (Viavi Solutions, San-Jose, CA, USA) source based on a semiconductor laser was used. This source has a number of necessary automatically supported measurement functions, including automatic stabilization of light wave radiation in the range of 900–1625 nm, as well as the Auto-λ and Multi-λ functions, which are essential for achieving measurement accuracy. The instruments were used to set up and calibrate the system. The connection to the OF was made through a universal UPP 2.5 mm adapter and optical connectors (OC) of the SC type.

Figure 3 shows a photograph of the used tension measurement instrument (TMI) with an accuracy of 0.01 mm.

Figure 3. Device for measuring displacements (minimum one division value).

An experimental setup was developed for the experiment (Figure 4). The experiment was carried out as follows. The displacement was performed by tightening the turnbuckles (TB) and nut bolt (NB) and measured by TMI. When displaced, the ends of the ferrules

into which the OF was inserted diverged by up to 30 mm; if needed, the measurement range can be extended to 100 mm. So far, there are limitations associated with the parameters of the used ferrules, which edged the ends of the OF through OC and the tube in which the ferrules move. Several sensors can be connected in series or used as a transmission mechanism to increase the divergence distance of the OF. Changes in the properties of light occur in relation to the intensity and phase of propagation when the ends of the OF move away from each other. It is reflected in changing the shape of the light spot. The farther the OF ends diverge from each other, the greater the level of additional losses and loss of optical power are. All the changes are recorded by the hardware-software complex and displayed on the screen.

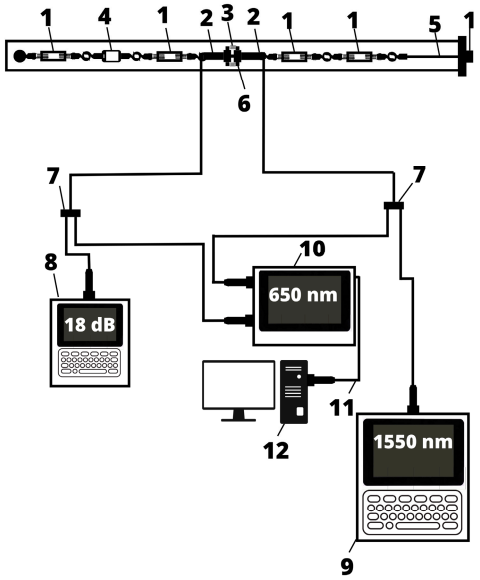

Figure 4. Graph obtained from the developed software, where 1 is the turnbuckle, 2 is the optical connector, 3 is the spring, 4 is the tension measurement instrument, 5 is the tension stud, 6 is the fiber -optic sensor of shift, 7 is the optical splitter, 8 is the optical power measurement instrument, 9 is the signal generator, 10 is the data processing device, 11 is the USB cable and 12 is the personal computer.

The data processing device (DPD) contains an optical radiation source, which is a semiconductor laser with the wavelength of 650 nm and power of 30 mW. In the DPD, there is a high-resolution photomatrix that perceives all the changes in the light wave during mechanical impact on the OF. The principle of operation of the data processing unit is based on controlling the changes in the properties of the light wave passing through the OF, followed by the analysis of changes in its intensity. The laser beam passes from the radiation source through the optical splitter (OS) and connecting patch cord to FOSS.

The OF ends diverge inside the ferrule and form additional losses in the event of a displacement, which leads to changing the intensity of the light spot incident on the surface of the photomatrix.

Multiple plastic sheaths and Kevlar thread were used to better protect the optical fiber from mechanical damage. This thread protects the fiber from breaking. The optical fiber was coated on top with a layer of acrylic varnish 100 microns thick, then a plastic sheath 0.9 mm thick and an additional sheath with a diameter of 3 mm were placed. This scheme for protecting the sensor from mechanical damage has been tested many times in practice and is quite effective. In the future, it is planned to improve this scheme by using protective metal armored sleeves located from the sensor to the data block. This protection scheme is more effective and applies to many different external factors (weather conditions, animals, natural disasters, etc.) in comparison with existing protection schemes. At

the same time, an alarm is triggered if the fiber-optic patch cord is damaged. It is built into the system to check the functionality of the sensor. Because quarrying takes place in open areas away from residential areas, wild animals may be nearby and cause damage, for example, foxes may chew through the fiber-optic patch cord.

2.2. Hardware and Software

The light spot contains a significant amount of noise, and the amount depends on the laser radiation stability and the ambient temperature. The OF has a stepped profile of the light spot, obeying the Gaussian distribution. The principle of data processing is to analyze the change in the profile of the light spot against the background of OF noise. Under mechanical action on the OF, the picture changes dramatically, which is perceived by the program, while the noise pollution is not taken into account. Great importance is given to the hardware-software complex for data processing, which is able to exclude temporal fluctuations and track the rate of changing the transition of pixels from black to white.

The hardware part of the system for monitoring the technical condition of the territory for mining operations using FOS was built on the principle of an open architecture and consists of three main parts: a coherent optical signal generator (laser), a FOS and a computing device that has the functions of receiving, processing and transmitting the data (Figure 5). Moreover, for the first two, well-known instruments were used, and the third part was built for the intellectual analysis in order to optimize the measurement process and costs.

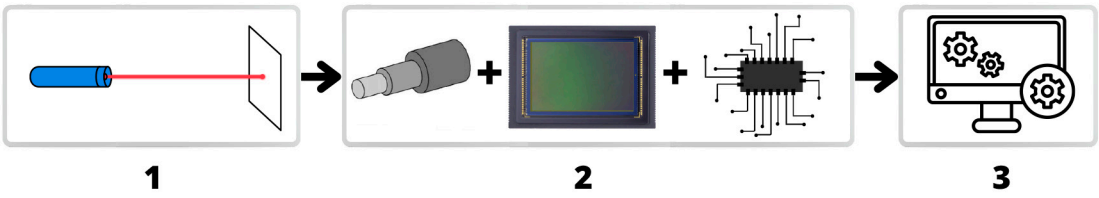

Figure 5. Structural diagram of the monitoring system.

The first part of the system generates an optical signal. When propagating through the OF, it changes its properties. As a result, the pattern of the light spot incident on the photomatrix also changes. The number of pixels in the picture was chosen as the parameter under consideration. The second part measures the number of pixels of the light spot, the nature of which changes when exposed to the OF. As a result, a digital signal is generated at the output of the measuring part, which is then processed by the third part. The displacement value is determined, which is displayed on the program screen based on the obtained data.

The image of the light spot at the output from the OF, shown in Figure 6, has a more illuminated region in the middle (1), in the interface (2) and in the region of losses emerging through the fiber cladding (3). A transition region is formed at the boundary, in which noise fluctuations are most clearly observed. These fluctuations can cause a violation of the adequacy of the obtained measurement data and cause a significant error in the obtained values.

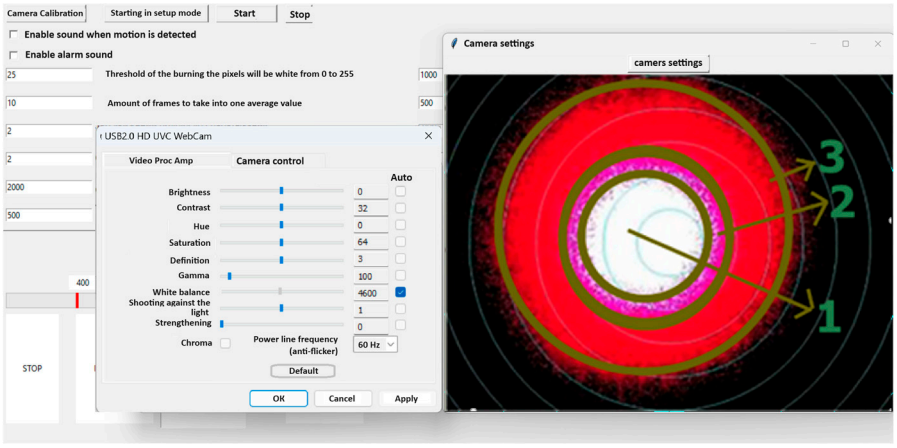

Figure 6. The program's appearance.

Software was developed in order to control the displacement parameters and to process them intelligently for improving the accuracy and reducing the likelihood of false alarms. The intelligence of the system lies in its ability to learn on the basis of the mechanical effects exerted on the FOS and make a decision on a warning alert about a possible violation of the integrity of the technological object. Moreover, it is possible to control the technical condition of up to several thousand reference stations simultaneously. However, the proposed algorithm is very complex. Thus, the cost of the device of the monitoring system is increased. It should be noted that the price also includes many years of research work. As a result, the fiber-optic monitoring system (FOSM) generates a fairly high cost.

An important factor is also that the mining safety control system in open pits is currently not equipped to use more than four physical channels. The main reason for this shortcoming is limitation of the computing power of the computer and the performance of the video card. Moreover, the physical number of channels is limited to four due to the limited computing capacity of the computer and the performance of the video card, as well as the created program algorithms, but in the future, their number will be increased to the real needs of the enterprise. Increasing the number of channels will definitely increase the cost, primarily due to increasing the length of the fiber-optic control cables, but safety issues are a higher priority.

The software for the open pit monitoring system for mining monitors the displacement of the pit walls is based on changing the number of pixels. The useful signal is separated from interference and noise generated by various impacts based on the developed algorithm, for example, temperature changes, as well as mechanical vibrations caused by the operation of equipment or people; moreover, when using the machine learning technology based on new data obtained during operation, the system learns, reducing the error of determination.

The hardware-software complex is able to track the rate of change in the derivative of the light wave intensity in time, as well as changes in the shape of the spot and the transition of pixels from white to black.

The system can also stepwise change its sensitivity. Initially, it is set to the maximum sensitivity to control the initial displacements and to give warning signals to the operator, after which the parameters are automatically coarsened for accurate fixing the displacement and eliminating false measurements.

The system is able to control changing rock pressure and displacements of roof rocks by changing the level of additional losses and changing the intensity of the light wave incident on the surface of the photodetector. Intelligent processing of the spot image makes it possible to track changes in the intensity of individual pixels. Figure 7 shows a window with images of light spots in a calm and disturbed state under mechanical action on the FOS. On the computer screen, it can be clearly seen how the light spot changes, especially at the interface between the core and the cladding of the OF. The light falling

on the surface of the television matrix contains a significant amount of noise. At the output of the OF, a light spot is formed, which falls on the surface of the television matrix and obeys the normal Gaussian distribution.

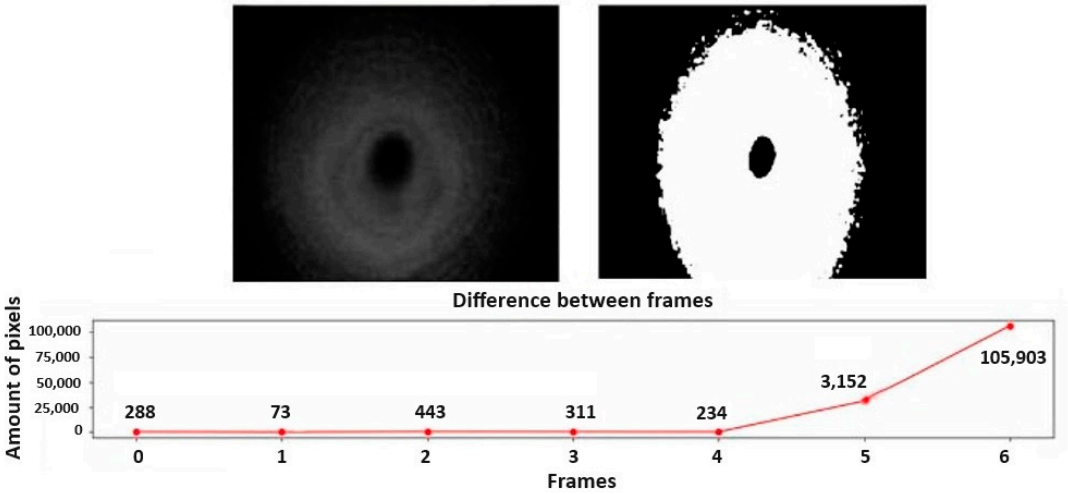

Figure 7. Plot obtained from the developed software.

The noise negatively affects the measurement process, but the program monitors the dynamics of changes in the shape of the light spot and is able to separate fluctuations caused by external factors, such as thermal effects on the OF, from useful signals. The operation of the system is partially based on the effect of photoelasticity and changing additional losses during mechanical action on the OF.

The program has several windows for configuration and operation. During operation, the screen displays not only the numerical values of the load, by which the displacement is calculated, but there are also the signal indicators of green, yellow and red colors, which are needed to warn of danger or vice versa about the normal operation of the system. With a sharp fluctuation in pressure and increasing the displacement parameter, a warning signal is given, and a yellow indicator turns on, indicating that the roof rocks have begun to move due to increasing rock pressure.

3. Results

The experiments were carried out by two methods. The first method controlled changing the intensity of the light spot and changing the pixel pattern when a displacement occurred.

The number of the pixels increased as the OF diverged (Figure 8).

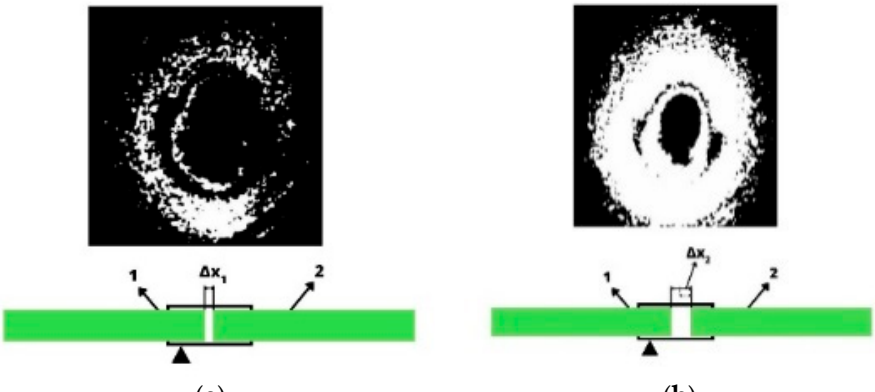

(**a**) (**b**)

Figure 8. Changing the number of spots with displacement of the optical fiber ends: (**a**) position 1; (**b**) position 2.

The plot of the number of pixels dependence on displacements is shown in Figure 9.

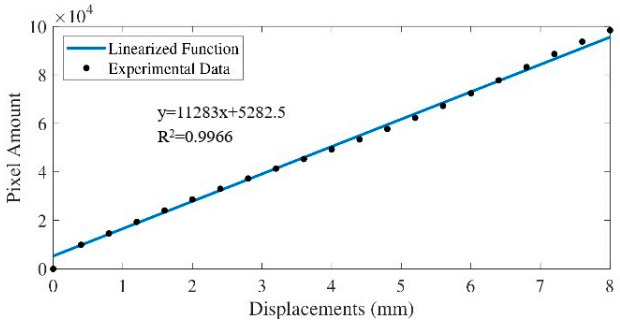

Figure 9. Number of pixels dependence on displacement.

To improve reliability of the results, they were verified by the second method, which consists of controlling additional losses using an optical power meter. When a displacement occurred, increasing additional losses was recorded. In both experiments, an almost linear dependence was obtained, which made it possible to construct a sufficiently accurate sensor for measuring displacements depending on the change in the properties of the light wave passing through the fiber core when their ends diverged inside the optical ferrule.

A plot of optical loss versus displacement is shown in Figure 10.

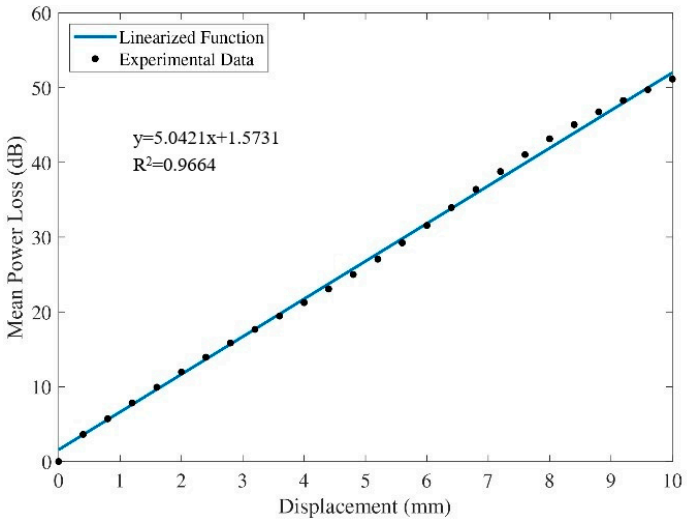

Figure 10. Optical loss dependence on displacements.

An automatic approximation of the experimental results was carried out, and it was found that the best mathematical model for numerical optimization is a linear approximation of the measurement results. As a result, the laboratory sample of the fiber-optic sensor showed a fairly high degree of linearity. An absolute error of 2.31, a relative error of 6.21% and a Student's coefficient of 2.120 with a confidence interval of 0.94 were calculated based on the measurement results. The hardware and software complex was designed to monitor rock displacements and crack expansions by such a parameter as an increase in additional losses in FOS, which is converted into a change in the number of pixels. The larger the offset is, the more white pixels are generated, so the calculated accuracy satisfies the

production requirements. It is important to control not only the exact numerical parameters of its expansion but also the growth of the crack. Measures to improve the accuracy of measurements with modification of designs to reduce the influence of external interference on their operation will be taken in further experiments.

A fiber-optic quarry collapse prevention monitoring system was installed at the Kenzhem quarry of AK Altynalmas JSC (Kazakhstan) for testing (Figure 11).

Figure 11. Implementation of a monitoring system in production.

Currently, this enterprise uses only mechanical monitoring and visual inspection methods with the participation of surveyors without the use of expensive equipment. At the moment, the sensors and control systems developed by the authors are undergoing comprehensive industrial tests, based on the results of which detailed schemes for the expanded implementation of data from fiber-optic rock condition monitoring systems will be developed, which is the subject of future research.

4. Discussion

According to the results of the experiments, an automatic approximation was carried out; the best mathematical model was a linear approximation. As a result, the laboratory sample of the fiber-optic sensor showed a fairly high linearity. The absolute error of 2.31, the relative error of 6.21% and the Student's coefficient of 2.120 were calculated with the confidence interval of 0.94 based on the measurement results.

5. Conclusions

The aspects of developing systems for monitoring the technical condition of opencast mines were defined, as well as other extended objects in the course of the study. The updated solutions related to this topic were analyzed. There are known methods of determining the displacement of stone slabs using FOS and methods of reflectometry and interferometry. Moreover, the use of artificial intelligence technology makes it possible to increase the measurement accuracy of FOSs.

The main idea of using systems for monitoring the technical condition of rocks based on fiber-optic mechanical displacement sensors is aimed at reducing the cost per measuring point. Currently, the cost of electronic displacement sensors is quite high, and many companies carry out monitoring using mechanical reference stations, as well as visual and instrumental observations with the participation of surveyors. The cost of the developed sensor is not much higher than the cost of the reference station, but at the same time, it allows for remote monitoring. The proposed sensors are a good alternative to expensive methods that use ground penetrating radar or satellite geoscanning.

The proposed solution based on a DFOS operating according to a new method and artificial intelligence makes it possible to solve the production safety problems of mining operations at the Kenzhem open pit of the Altynalmas JSC (Kazakhstan). The violation of the integrity of stone slabs cannot only be determined, but possible emergency situations can also be predicted. The use of FOMS of a distributed type will allow for the remote controlling stability of the pit walls in real time. The obtained results of the laboratory

studies allow us to state that the developed FOS has a fairly good linearity of characteristics and low power consumption at a distance of 30÷50 km compared to electrical measuring systems. Developing the own circuit solutions and hardware and software complex, as well as the use of standard telecommunications equipment, radiation sources, photodetectors, fiber-optic cables and connectors can significantly reduce the cost of FOSM as a whole.

This development is universal and can be applied to any mining enterprises, regardless of the structure and properties of the rocks. The cost of one sensor, which makes it possible to monitoring a working area up to 3 m wide, is approximately USD 150; the cost of the hardware and software complex is about USD 2000. Connecting up to 16 sensors is possible to one hardware and software complex. The number of sensors depends on the width of the face where the mining equipment operates and ranges from 16 to 32 sensors with a working area of about 100 m, depending on the conditions. In the future, it is planned to improve the designs of sensors and algorithms of the hardware and software complex, which will reduce the cost of the system during mass production.

Unlike the existing solutions, the proposed one has an error of 6.21% at a relatively cheap cost. Further studies will consider improving the system to increase the number of physical measuring channels, as well as optimizing the computational processes.

When developing a fiber-optic quarry collapse prevention monitoring system, a variety of criteria were used, which can vary depending on the specific application, context and requirements. However, there are some fundamental criteria that are usually taken into account: continuous monitoring of changes in deformation that lead to displacement of the rock mass and the development of cracks and prevention of possible pit wall failures. One of the main advantages is the system's ability to provide accurate results in laboratory tests or in real mining conditions.

Unlike existing monitoring systems, the implemented fiber-optic monitoring system for preventing quarry collapses is an inexpensive and simple solution, characterized by low cost and ease of operation (replacement, repair and modernization). The developed theoretical foundations of optoelectronic processes in an optical fiber loaded with external mechanical influences will make possible in the future to develop a universal hardware-software complex that allows one to study properties with a high degree of mathematical accuracy and predict various mechanical rocks changes (deformation, destruction, etc.) in a wide range of temperature parameters and mechanical stresses for various kinds of mineralogical structures operating in extreme conditions. The system makes it possible to monitor rock displacement readings remotely and with the help of GPS navigation methods and is characterized by lower economic costs compared to existing systems. The system is more energy efficient and operates on the basis of energy-saving electrical elements in the form of solar panels. The use of fiber-optic sensors is less economically expensive and more environmentally friendly, in comparison with existing control and measuring systems based on electronic sensors, characterized by the rather high cost of laying a separate cable line and the need for rather expensive measures to move the face and dismantle the power supply.

Author Contributions: Conceptualization, Y.N., V.K. and N.K.; data curation, Y.N., A.M., N.K. and I.K.; formal analysis, A.M., V.K., N.K., O.G. and I.K.; investigation, A.M., V.K. and I.K.; methodology, Y.N., V.K. and O.G.; project administration, Y.N.; resources, Y.N., A.M., N.K. and O.G.; software, N.K., O.G. and I.K.; supervision, Y.N.; validation, Y.N., A.M., V.K., N.K. and I.K.; visualization, O.G. and I.K.; writing—original draft, Y.N., A.M. and V.K.; writing—review and editing, Y.N., A.M., V.K. and O.G. All authors have read and agreed to the published version of the manuscript.

Funding: This research is funded by the Science Committee of the Ministry of Science and Higher Education of the Republic of Kazakhstan (Grant No. AP14869145 "Development of an intelligent fiber-optic system for monitoring the geotechnical condition of mining pits and sections").

Institutional Review Board Statement: Not applicable.

Informed Consent Statement: Not applicable.

Data Availability Statement: The original contributions presented in the study are included in the article.

Acknowledgments: The authors thank the administration of the Abylkas Saginov Karaganda Technical University, the Saken Seifullin Kazakh Agro Technical Research University and the Tomsk Polytechnic University.

Conflicts of Interest: The authors declare no conflicts of interest.

References

1. Mekhtiyev, A.D.; Neshina, E.G.; Madi, P.; Gorokhov, D.A. Automated fiber-optic system for monitoring the stability of the pit quarry mass and dumps. *Occup. Saf. Ind.* **2021**, *4*, 19–26. https://doi.org/10.24000/0409-2961-2021-4-19-26.
2. Mekhtiyev, A.D.; Yurchenko, A.V.; Ozhigin, S.G.; Neshina, E.G.; Al'kina, A.D. Quasi-distributed fiber-optic monitoring system for overlying rock mass pressure on roofs of underground excavations. *J. Min. Sci.* **2021**, *57*, 354–360. https://doi.org/10.1134/S1062739121020198.
3. Kulikov, V. Fiber-optic perimeter security system on Bragg gratings, as a promising method of monitoring the security of the facility. *Polzunov's Alm.* **2010**, *2*, 274–278. Available online: http://elib.altstu.ru/journals/Files/pa2010_2/pdf/274kulikov.pdf (accessed on 9 January 2024). (In Russian)
4. Tomyshev, K.A.; Bagan, V.A.; Astapenko, V.A. Distributed fiber-optic pressure sensors for use in the oil and gas industry. *Proc. MIPT* **2012**, *4*, 64–72. Available online: https://old.mipt.ru/upload/394/f_g7ce-arphcxl1tgs.pdf (accessed on 9 January 2024). (In Russian)
5. Lanciano, C.; Salvini, R. Monitoring of Strain and Temperature in an Open Pit Using Brillouin Distributed Optical Fiber Sensors. *Sensors* **2020**, *20*, 1924. https://doi.org/10.3390/s20071924.
6. Payawal, J.M.G.; Kim, D.-K. Image-Based Structural Health Monitoring: A Systematic Review. *Appl. Sci.* **2023**, *13*, 968. https://doi.org/10.3390/app13020968.
7. Wang, Y.; Yuan, H.; Liu, X.; Bai, Q.; Zhang, H.; Gao, Y.; Jin, B. A Comprehensive Study of Optical Fiber Acoustic Sensing. *IEEE Access* **2019**, *7*, 85821–85837. https://doi.org/10.1109/ACCESS.2019.2924736.
8. Udd, E. The Emergence of Fiber-optic Sensor Technology. In *Fiber-Optic Sensors: An Introduction for Engineers and Scientists*, 2nd ed.; Udd, E., Spillman, W.B., Eds.; Wiley: Hoboken, NJ, USA, 2011; p. 1. https://doi.org/10.1002/9781118014103.ch1.
9. Sánchez, L.A.; Díez, A.; Cruz, J.L.; Andrés, M.V. Recent Advances in Forward Brillouin Scattering: Sensor Applications. *Sensors* **2022**, *23*, 318. https://doi.org/10.3390/s23010318.
10. Zheng, H.; Zhang, J.; Guo, N.; Zhu, T. Distributed Optical Fiber Sensor for Dynamic Measurement. *J. Light. Technol.* **2021**, *39*, 3801–3811. https://doi.org/10.1109/JLT.2020.3039812.
11. Fu, J.; Guo, Y.; Li, P. A Fiber Bragg Grating Anchor Rod Force Sensor for Accurate Anchoring Force Measuring. *IEEE Access* **2020**, *8*, 12796–12801. https://doi.org/10.1109/ACCESS.2020.2966235.
12. Nagulapally, P.; Shamsuddoha, M.; Rajan, G.; Mohan, M.; Prusty, B.G. Distributed Fiber-optic Sensor-Based Strain Monitoring of a Riveted Bridge Joint Under Fatigue Loading. *IEEE Trans. Instrum. Meas.* **2021**, *70*, 6009610. https://doi.org/10.1109/TIM.2021.3101324.
13. Wu, Y.; Zhang, Y.; Wu, J.; Yuan, P. Fiber-Optic Hybrid-Structured Fabry–Perot Interferometer Based On Large Lateral Offset Splicing for Simultaneous Measurement of Strain and Temperature. *J. Light. Technol.* **2017**, *35*, 4311–4315. https://doi.org/10.1109/JLT.2017.2734062.
14. Dong, Y.; Ren, G.; Xiao, H.; Gao, Y.; Li, H.; Xiao, S.; Jian, S. Simultaneous Temperature and Strain Sensing Based on M-Shaped Single Mode Fiber. *IEEE Photonics Technol. Lett.* **2017**, *29*, 1955–1958. https://doi.org/10.1109/LPT.2017.2757933.
15. Subramanian, R.; Zhu, C.; Zhao, H.; Li, H. Torsion, Strain, and Temperature Sensor Based on Helical Long-Period Fiber Gratings. *IEEE Photonics Technol. Lett.* **2018**, *30*, 327–330. https://doi.org/10.1109/LPT.2017.2787157.
16. Du, C.; Tang, Q.; Zhou, J.; Guo, X.; Yu, T.; Wang, X. Fiber-optic Sensors Based on Photoacoustic Effect for Rebar Corrosion Measurement. *IEEE Trans. Instrum. Meas.* **2019**, *68*, 4559–4565. https://doi.org/10.1109/TIM.2018.2890318.
17. Liu, T.; Wei, Y.; Song, G.; Hu, B.; Li, L.; Jin, G.; Wang, J.; Li, Y.; Song, C.; Shi, Z.; et al. Fibre optic sensors for coal mine hazard detection. *Measurement* **2018**, *124*, 211–223. https://doi.org/10.1016/j.measurement.2018.03.046.
18. Ren, F.; Zhang, W.; Li, Y.; Lan, Y.; Xie, Y.; Dai, W. The Temperature Compensation of FBG Sensor for Monitoring the Stress on Hole-Edge. *IEEE Photonics J.* **2018**, *10*, 7104309. https://doi.org/10.1109/JPHOT.2018.2858847.
19. Li, T.; Shi, C.; Ren, H.; Novel, A. Fiber Bragg Grating Displacement Sensor with a Sub-Micrometer Resolution. *IEEE Photonics Technol. Lett.* **2017**, *29*, 1199–1202. https://doi.org/10.1109/LPT.2017.2712602.
20. Su, J.; Dong, X.; Lu, C. Property of Bent Few-Mode Fiber and Its Application in Displacement Sensor. *IEEE Photonics Technol. Lett.* **2016**, *28*, 1387–1390. https://doi.org/10.1109/LPT.2016.2542366.
21. Kim, S.-T.; Park, Y.-S.; Yoo, C.-H.; Shin, S.; Park, Y.-H. Analysis of Long-Term Prestress Loss in Prestressed Concrete (PC) Structures Using Fiber Bragg Grating (FBG) Sensor-Embedded PC Strands. *Appl. Sci.* **2021**, *11*, 12153. https://doi.org/10.3390/app112412153.

22. Kulchin, Y.N.; Kamenev, O.T.; Petrov, Y.S.; Kolchinsky, V.A. Fiber-optic interferometric receivers of weak seismic signals. *Vestn. Far East. Branch Russ. Acad. Sci.* **2016**, *4*, 56–59. (In Russian)
23. Garcia-Souto, J.A.; Lamela-Rivera, H. Comparative analysis of optical-fibre interferometric sensors versus accelerometers: Application to vibrations inside high-power transformers. *J. Opt. A Pure Appl. Opt.* **2002**, *4*, 318–326. https://doi.org/ 10.1088/1464-4258/4/6/375.
24. Gardner, D.L.; Hofler, T.; Baker, S.R.; Yarber, R.K.; Garrett, S.L. A fiber-optic interferometric seismometer. *J. Light. Technol.* **1987**, *5*, 953–960. Available online: https://core.ac.uk/download/pdf/36736238.pdf (accessed on 9 January 2024).
25. Kim, S.; Park, Y.; Park, S.; Cho, K.; Cho, J.-R. A Sensor-Type PC Strand with an Embedded FBG Sensor for Monitoring Prestress Forces. *Sensors* **2015**, *15*, 1060–1070. https://doi.org/10.3390/s150101060.
26. Dandridge, A. Fiber-optic Sensors Based on the Mach–Zehnder and Michelson Interferometers. In *Fiber-Optic Sensors: An Introduction for Engineers and Scientists*, 2nd ed.; Udd, E., Spillman, W.B., Eds.; Wiley: Hoboken, NJ, USA, 2011; p. 231. https://doi.org/10.1002/9781118014103.ch10.
27. Kamenev, O.T.; Kulchin, Y.N.; Petrov, Y.S.; Khizhnyak, R.V. Application of the Mach-Zender fiber−optic interferometer for the creation of long-base deformometers. *Tech. Phys. Lett.* **2014**, *40*, 49–56. (In Russian)
28. Zhao, Y.; Zhang, N.; Si, G. A Fiber Bragg Grating-Based Monitoring System for Roof Safety Control in Underground Coal Mining. *Sensors* **2016**, *16*, 1759. https://doi.org/10.3390/s16101759.
29. Mekhtiyev, A.D.; Yurchenko, A.V.; Kalytka, V.A.; Neshina, Y.G.; Alkina, A.D.; Madi, P.S. A Fiber-Optic Long-Base Deformometer for a System for Monitoring Rocks on the Sides of Quarries. *Tech. Phys. Lett.* **2022**, *48*, 30–32. https://doi.org/10.21883/PJTF.2022.15.53129.19200.
30. Kalytka, V.A.; Korovkin, M.V.; Mekhtiev, A.D.; Yurchenko, A.V. Non-linear polarizing effects in dielectrics with hydrogen bonds. *Russ. Phys. J.* **2018**, *61*, 757–769. https://doi.org/10.1007/s11182-018-1457-8.
31. Li, S.; Ren, S.; Chen, S.; Yu, B. Improvement of Fiber Bragg Grating Wavelength Demodulation System by Cascading Generative Adversarial Network and Dense Neural Network. *Appl. Sci.* **2022**, *12*, 9031. https://doi.org/10.3390/app12189031.
32. Zinsou, R.; Wang, Y.; Liu, X.; Bai, Q.; Wang, Y.; Jin, B. Adaptive Pulse Period Method for Low-Frequency Vibration Sensing With Intensity-Based Phase-Sensitive OTDR Systems. *IEEE Access* **2020**, *8*, 41838–41846. https://doi.org/10.1109/ACCESS.2020.2977000.
33. Sun, Y.; Li, X.; Ren, C.; Xu, H.; Han, A. Distributed Fiber-optic Sensing and Data Processing of Axial Loaded Precast Piles. *IEEE Access* **2020**, *8*, 169136–169145. https://doi.org/10.1109/ACCESS.2020.3023626.
34. Wu, H.; Wan, Y.; Tang, M.; Chen, Y.; Zhao, C.; Liao, R.; Chang, Y.; Fu, S.; Shum, P.P.; Liu, D. Real-Time Denoising of Brillouin Optical Time Domain Analyzer with High Data Fidelity Using Convolutional Neural Networks. *J. Light. Technol.* **2019**, *37*, 2648–2653. https://doi.org/10.1109/JLT.2018.2876909.
35. Mekhtiyev, A.D.; Aimagambetova, R.Z.; Aubakirova, B.B.; Khozhas, A.K.; Madi, P.S.; Alkina, A.D.; Sarsikeyev, Y.Z.; Mekhtiyev, R.A. Fiber-Optic Security Signaling System for Preventing Emergency Failure of Reinforced Concrete Structures and Any Extended Objects. KAZ Patent 7 775, 27 January 2023.
36. Mekhtiyev, A.D.; Alkina, A.D.; Madi, P.S.; Aimagambetova, R.Z. Automated Fiber-Optic System for Monitoring, Telemetry and Control of Stationary Objects, Water Bodies and Earthquake-Prone Areas. KAZ Patent 36 074, 27 January 2023.
37. Kalytka, V.A.; Korovkin, M.V.; Aliferov, A.I.; Bashirov, A.V.; Talaspekov, D.R. The scheme of numerical optimization of the parameters of electrophysical processings in heterogeneuos solid elements. *Bull. Karaganda Univ. Phys. Ser.* **2018**, *90*, 34–41. Available online: http://rep.ksu.kz/handle/data/3692 (accessed on 10 January 2024).